Received: 08 January 2024 | Revised: 19 February 2024 | Accepted: 29 February 2024
DOI: 10.48309/JMPCR.2024.434706.1081
Journal of Medicinal and Pharmaceutical Chemistry Research
SAMI

FULL PAPER

Synthesis, characterization, anticorrosion, and computational study of new thiadiazole-oxadiazole derivatives with some transition metal ion

Amal H. Anatheil[a] |Azhar Hameed Gatea[b] |Fayez Owaid Neamah [c,*]

[a]*Department of Pharmaceutical Chemistry, College of Pharmacy, University of Thi-Qar, 64001, Thi-Qar, Iraq*

[b]*Department of Pathological Analytics Science, College of Applied Medical Science, Shatrah University, Thi-Qar, 64001, Thi-Qar, Iraq*

[c]*Directorate-General for Education Dhi Qar, Nassiriya 64001, Iraq*

***Corresponding Author:**
Fayez Owaid Neamah
Email: fayezawid@utq.edu.iq
Tel.: + 9647721014811

2,2'-((1,3,4-Thiadiazole-2,5-diyl)bis(hydrazine-2,1-diyl))bis(1,3,4-oxadiazole-5, 2-diyl) is a novel heterocyclic ligand. Diphenol was produced together with its compounds with Cu(II), Ni(ll), and Co(ll). The ^{1}H-NMR, mass, Fourier transform infrared (FT-IR), magnetic susceptibility, atomic absorption, elemental analysis [C, H, N, and S], conductance studies, and other factors have all been used to describe the ligand and its complexes. In a 1 M HCl solution, the ligand's ability to prevent carbon steel alloy corrosion was evaluated. The weight loss technique was used to measure the corrosion inhibition effectiveness. It was discovered that the inhibitor and the Fe^{2+} ion formed a combination. However, at B3LYP/6-311++G level of theory, quantum chemical calculations were carried out utilizing the DFT approach. Theoretical and experimental findings were found to be in excellent agreement. The electrostatic potential of the produced compounds was studied using the PM3 technique and the Hyperchem 8.02 software for theoretical accounting.

KEYWORDS

Ligand; complexes; characterization; anti-corrosion; hyperchem; electrostatic potential.

Introduction

Heterocyclic compounds are those that are cyclic and include atoms from at least two distinct elements in their ring members [1]. Sulfur, oxygen, and nitrogen are the most prevalent heteroatoms [2]. Heterocyclic compound chemistry is an intriguing area of research. Heterocyclic compounds fall into two categories: thiadiazole and oxadiazole. A cyclic molecule with one oxygen and two nitrogen atoms arranged in five-membered ring is called an oxadiazole [3].

Thiadiazole is a heterocyclic molecule with an aromatic five-membered ring that contains one sulfur atom and two nitrogen atoms. It was discovered that a number of significant pharmacophores implicated in diverse activities [4].

In medicinal chemistry, heterocyclic molecules are essential and have piqued strong interest due to their ability to process and synthesize a greater range of pharmacological and biological characteristics [5-7]. Additionally, they may be used as copolymers, sanitizers, developers, antioxidants, and

corrosion inhibitors [8,9] and pigment in addition to fluorescence components [10].

Experimental

Synthesis of 2-hydroxy benzohydrazides

A combination of methyl benzoate (15.2 mL, 0.1 mol) and hydrazine monohydrate (7.5 mL, 0.15 mol) in ethanol absolute (25 mL) was used to begin the production. After refluxing the combination for six hours, it was cooled, filtered, evaporated to half its volume, and then recrystallized from ethanol absolute [11]. With a yield of 90% and a melting point of 150 °C, the solid product was pale white in color.

Synthesis of 2-(5-mercapto-1,3,4-oxadiazol-2-yl)phenol

Two-hydroxybenzohydrazide (15.2 gm, 0.1mol), carbon disulfide (7.6 mL, 0.1 mol), and potassium hydroxide (5.6 g, 0.1mol) refluxed in 40 milliliters of pure ethanol. After the solvent was evaporated and acidified with 10% HCl, the resultant solid was recrystallized from ethanol absolute [12]. After that, the precipitate was filtered. The yellow solid had a 70% yield and a melting point of 200 °C.

Synthesis of 1,3,4-thiadiazole-2,5-dithiol

For twenty-five hours, a combination of (80%) carbon disulfide (0.2 mol, 15 g), KOH (0.2 mol, 11 g), and hydrazine hydrate (0.1 mol, 5 g) was refluxing. TLC responded to the response. Hydrochloric acid (10%) was used to separate the resultant solid after the surplus solvent was distilled off. After the mixture was filtered, the ethanol was recrystallized as a dark yellow solid. (162-164) ◦ C for m.p., 65% yield [13].

Synthesis2,5-dihydrazinyl-1,3,4-thiadiazole

For 16 hours, a combination of 0.1 mol, 15g of 1,3,4-thiadiazole-2,5-dithiol, 40 mL of 100% ethanol, and (99%) 0.2 mol, 10 g of hydrazine hydrate was refluxed. After the reaction, TLC was used. After the product had reached room temperature, 100 milliliters of ice water was added. After filtering, washing with water, and recrystallizing the yellow solid product from ethanol, the yield was 72% [14].

Synthesis2,2'-(((1,3,4-thiadiazole-2,5-diyl)bis(hydrazine-2,1-diyl))bis(1,3,4-oxadiazole-5,2-diyl))diphenol

The ligand was created by condensing 2-(5-mercapto-1,3,4-oxadiazol-2-yl)phenol (13.2 g, 0.068 mol) and 2,5-dihydrazinyl-1,3,4-thiadiazole (5 g, 0.034 mol) at a ratio of 1:2 molar in (40 mL) pure ethanol. Next, under TLC supervision, the mixture refluxed for 20 hours. A white ligand with a melting point of 228-230 °C and a yield of 65% was obtained by precipitating, filtering, and recrystallizing the ligand in ethanol absolute.

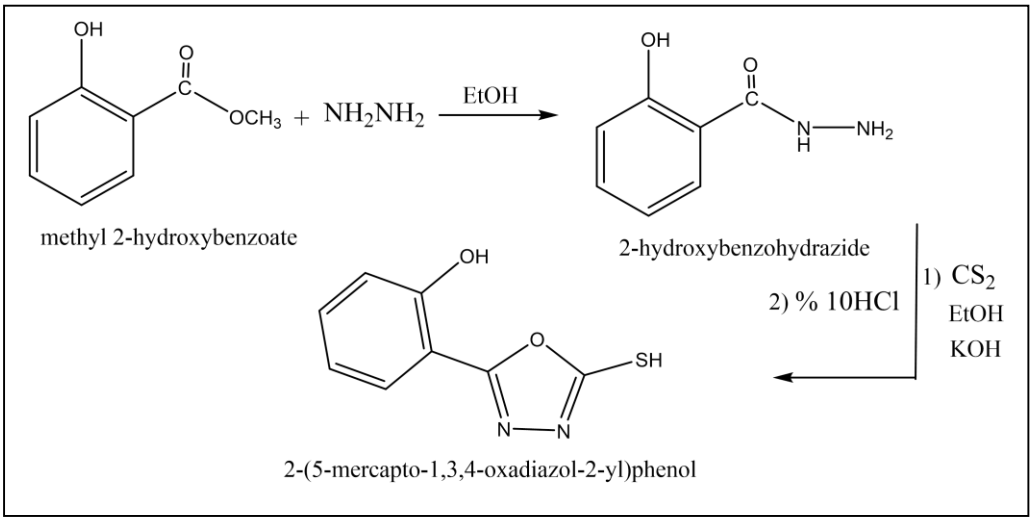

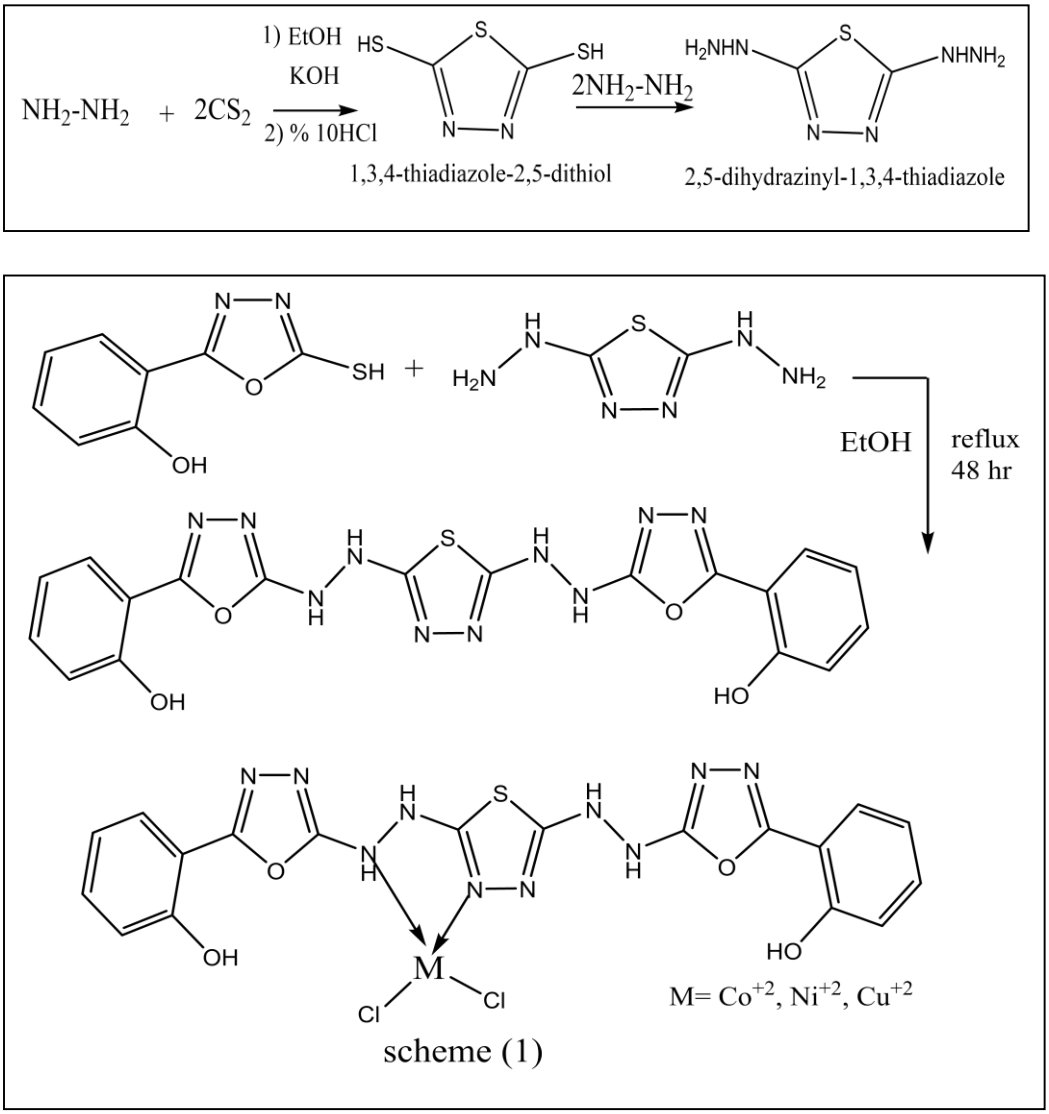

SCHEME 1 Synthesis of ligands and their complexes

Preparation of complexes

The complexes were created by combining ligand (0.001mol) with salts ($NiCl_2.6H_2O$, $CuCl_2.2H_2O$, and $CoCl_2.6H_2O$) separately in 30 milliliters of 100% ethanol, then refluxing the mixture for two hours while TLC observed the process. After filtering and repeatedly washing the precipitate with ethanol or aqueous ethanol to eliminate any remaining ligand or salts, the precipitated complexes were dried.

Results and discussion

The multistep synthetic procedure utilized to produce the ligand L is shown in Scheme 1. The 2-(5-mercapto-1,3,4-oxadiazol-2-yl)phenol was condensed with 3-2,5-dihydrazinyl-1,3,4-thiadiazole to provide the necessary ligand L.

Analysis and physical measurements

Physical properties and elementa microanalysis CHNS, magnetic susceptibility, atomic absorption and conductance measurements are indicated in Table 1.

TABLE 1 Physical properties and elemental microanalysis data

No.	Formula	Color	(C%)Ex. C% Cal.	(H%)Ex H% Cal.	(N%)ExN % Cal.	(S%)Ex. S% Cal.	Atomic absor. M%	Λ Scm² mol⁻¹	M.p °C	μeff B.M
1	$C_{10}H_{10}N_8O_2S$ (L)	Brown	(45.51) 46.35	(2.78) 3.03	(31.12) 30.03	(5.11) 6.87		-----	200	-----
2	$Cu(L)Cl_2$	Green					(13.05) 10.58	18	252	1.9
3	$Co(L)Cl_2$	Dark grey					(12.15) 9.88	22	239	4.8
4	$Ni(L)Cl_2$	Yellow					(10.76) 9.85	12	245	0.48

FT-IR spectra

FT-IR analysis of the synthesized ligand and its complexes was performed using CsI for complexes and KBr disc for the ligand. A distinctive stretching absorption band is seen in the ligand's FT.IR spectra at (3448)cm^{-1},(3348)cm^{-1}, (3026)cm^{-1}, (1625)cm^{-1}, (1527) cm^{-1}, (1327) cm^{-1}, and (1273) cm^{-1} [15] which are correspondingly related to the bands (υOH), (υNH), (υC-H)Aro, (υC=N), (υC=C), (υC-O-C), and (υC-S-C). The coordinated (M-N) and (M-Cl) bond-related complexes showed the formation of new bands in their spectra, which were located in the (504-578) cm^{-1} and (282-316) cm^{-1}, respectively. This suggests that the coordinate passed via the atoms of (N) and (Cl). The IR data are shown in Figures 16-19 and Table 2.

TABLE 2 L's and its metall complexes' infrared data (υ cm-1)

Assignment	υ(O-H)	υ(N-H)	υ(C-H) aro.	υ(C=N)	υ(C=C)	υ(C-O-C)	υ(C-S-C)	υ(N-M)	υ(M-Cl)
Ligand(L)	3448	3348	3062	1625	1527	1327	1126		
$[Co(L)Cl_2]$	3278	3093	3030	1635	1519	1334	1265	578	316
$[Ni(L)Cl_2]$	3286	3093	3020	1635	1519	1334	1265	578	316
$[Cu(L)Cl_2]$	3286	3170	3070	1604	1519	1334	1280	504	282

Nuclear magnetic resonance

According to Figure 11, the ligand's ^{1}H-NMR spectra show signals at (11.82 ppm, 2H), (10.91 ppm, 2H), (10.45 ppm, 2H), and (6.94-7.94 ppm, 8H) because of protons in the aromatic ring that connect to the oxadiazole ring, as well as (N-H)c,(N-H)b, and (O-H)a protons.

Mass spectra

The chemical formula C18H14N10O4S is consistent with the ligand's mass spectrum, which showed a molecular ion peak at 466 m/z. $[C18H13N10O3S]^+$ = 450 m/z, [C18H12N10O2S2]+ = 432 m/z, [C10H7N6O2S]+ = 275 m/z, [C8H5N2O2]+ = 176 m/z, [C10H8N7O2S]+ = 290 m/z, [C8H7N4O2]+ = 191 m/z, [C8H5N2O2]+ = 161 m/z, [C2H4N6S]+ = 145 m/z, and [CHNS]+ = 59 m/z base peak are the causes of the remaining peaks.

The Co(II) complexes' mass spectra revealed molecular ion peaks at 596 m/z that were associated with [Co(L)Cl2].+ the stoichiometry. Because of the loss of two chlorine atoms, this compound exhibits additional fragmentation peaks at 561 and 525 m/z, respectively.

The Ni(II) complexes' mass spectra revealed molecular ion peaks at 595 m/z, which are consistent with the [Ni(L)Cl2].+ stoichiometry. Due to the loss of two chlorine atoms, this compound exhibits additional fragmentation peaks at 560 and 525 m/z, respectively.

Cu(II) complexes' mass spectra revealed molecular ion peaks at 600 m/z that matched the [Ni(L)Cl2].+ stoichiometry. As shown in Figures 9-15, this complex exhibits further fragmentation peaks at 565 m/z and 529 m/z, respectively, as a result of the loss of two chlorine atoms.

Magnetic susceptibility

At room temperature, the magnetic susceptibility values of metal complexes are collected. Table 1 lists the magnetic momentum for every metal complex. These magnetic measurements provide insight into the transition metal ion of the complexes' electronic state. As anticipated given Square planer shape, the measured magnetic momentum value of the Cu(II) complex was 1.9 BM. Co(II) has a magnetic momentum value of 4.8 BM, indicating tetrahedral shape. For Ni(II), the corresponding square planar shape is suggested by 0.48 BM [17].

Molar conductivity measurements

The produced metal complexes' molar conductivity was measured at room temperature using DMSO as a solvent at a concentration of 10-3 M. Table 3 contains a list of the conductivity values (1). The nonionic structure and nonelectrolyte character of the Co(II), Ni(II), and Cu(II) complexes are shown by their molar conductance [18,19].

Anticorrosion inhibitor

Using weight loss techniques, the synthesized compounds' ability to suppress corrosion on carbon steel alloy in a 1 M HCl solution was examined. In a closed beaker, steel specimens measuring 2.5 cm × 5 cm × 0.5 cm were submerged in 1 M HCl for 3-15 hours at 30-60 °C, both with and without the addition of varying inhibitor doses. For every condition, specimens were exposed in triplicate, and the average weight losses were documented. Table 3 displays the contents of the steel specimens [3].

TABLE 3 Contents of steel specimens

Element	C	Si	Mn	P	S	Ni	Cr	Al	V	Ti	Cu	Fe
Weight (%)	0.19	0.05	0.94	0.009	0.004	0.014	0.009	0.034	0.016	0.003	0.022	Rest

The corrosion rate (k) was calculated from the following equation [20]:

$$K = \Delta W / St \quad mg/cm^2.h \quad (1)$$

Where, ΔW is the average weight loss of three parallel steel sheets, t is the immersion duration, and S is the specimen's total area. The following formula was used to get the surfactant area, IE%, and corrosion inhibition efficiency [21]:

$$IE\% = (CR_{uninh}-CR_{inh}/ CR_{uninh}) * 100 \quad (2)$$

$$\Theta = (CR_{uninh}-CR_{inh}/ CR_{uninh}) \quad (3)$$

Where, IE% = inhibition efficiency, CR_{uninh}= Corrosion Rate without inhibitor, and rCR_{inh}= Corrosion Rate with inhibitor.

Table 4 presents the weight loss results for carbon steel in (1) M HCl with and without different inhibitor concentrations. According to the findings, the manufactured inhibitor's efficacy in inhibiting corrosion rises as its concentration does, as shown in Figures 1 and 2. At 30, 40, 50, and 60 °C, the effect of temperature on the inhibitory efficiency was investigated. As shown in Figure 3, it was found that the inhibitory efficacy drops as temperature rises from 30 to 60 °C. The

decrease in inhibition efficacy with increasing temperature might be ascribed to the higher temperatures causing the inhibitor molecules to desorb from the metal surface. Iron and steel have been protected against acid corrosion by various organic compounds that include nitrogen, oxygen, or sulfur [22]. Ecologically advantageous inhibitors may be defined as molecules containing heteroatoms due to their low toxicity and high chemical activity. Organic molecules' adsorption characteristics are affected by a variety of factors, including sizes, electron density at the donor atoms, and the orbital structure of the donating electrons [23].

TABLE 4 Weight loss information for carbon steel corrosion in 1 M HCl both with and without various dosages of the artificially produced inhibitor at 30 °C

Conc.	Time	3 h	6 h	9 h	12 h	15 h
(1M) HCl	ΔW(g)	0.0083	0.0111	0.0172	0.0234	0.0286
	Rc $mgcm^{-2}h^{-1}$	0.227	0.153	0.156	0.157	0.152
20 ppm	ΔW(g)	0.0068	0.0094	0.0108	0.0145	0.0168
	Rc $mgcm^{-2}h^{-1}$	0.181	0.125	0.096	0.097	0.089
	%IE	20	18	38	38.2	41
	(Θ)	0.20	0.18	0.38	0.382	0.41
40 ppm	ΔW(g)	0.0051	0.0082	0.0093	0.0121	0.0144
	Rc $mgcm^{-2}h^{-1}$	0.136	0.109	0.084	0.081	0.078
	%IE	40	29	46	48	49
	(Θ)	0.40	0.29	0.46	0.48	0.49
60 ppm	ΔW(g)	0.0036	0.0068	0.0082	0.0105	0.0117
	Rc $mgcm^{-2}h^{-1}$	0.101	0.091	0.073	0.07	0.063
	%IE	56	41	53	55	59
	(Θ)	0.56	.41	0.53	0.55	.59

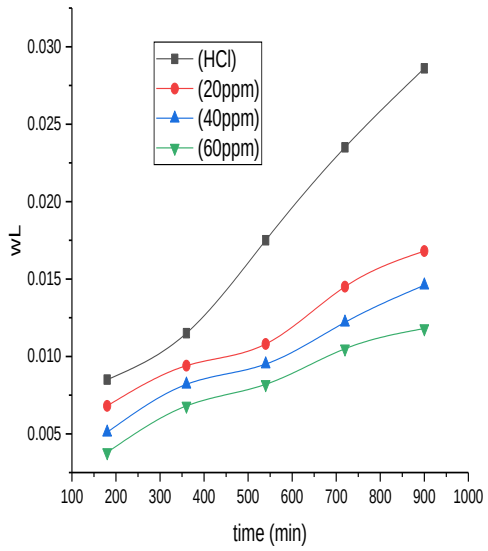

FIGURE 1 An anticorrosion inhibitor for carbon steel at 30 °C in 1M HCl with varying ligand concentrations

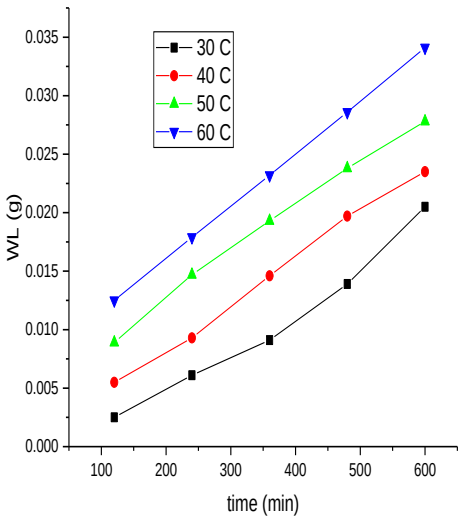

FIGURE 2 Anti-corrosion inhibitor of carbon steel in 1M HCl at varying temperatures with 20 ppm ligand concentration

Density Functional Theory at B3LYP (using Lee, Yang, and Parr's correlation functional with Becke's three-parameter hybrid functional), which incorporates both local and non-local terms correlation functional) techniques at 6-311++G level were used to do the theoretical calculations [24]. This computational study was carried out using the Gaussian 09 software package [25]. The process that looks for the molecule's minimal energy configuration is known as geometry optimization. The process finds a new geometry with a lower energy after calculating the wave function and energy at an initial geometry.

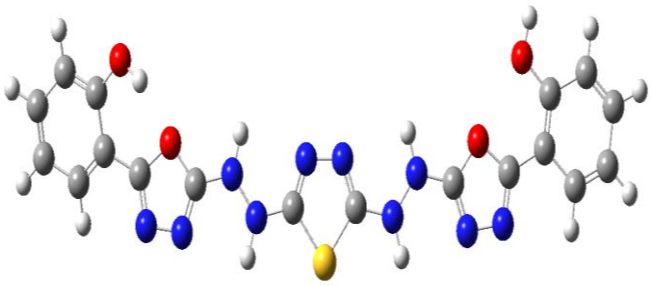

FIGURE 3 The optimized structure of the ligand

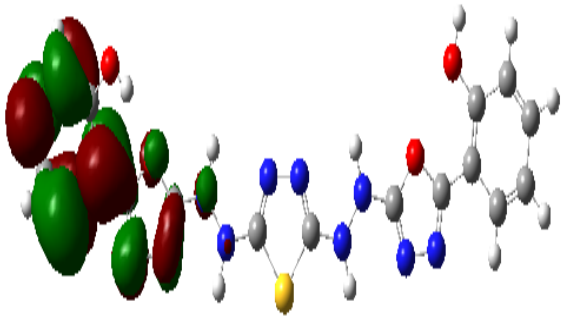

FIGURE 4 LUMO orbital

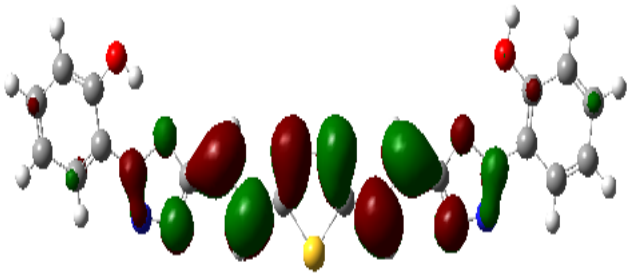

FIGURE 5 HOMO orbital

For physicists and chemists, molecular orbitals (HOMO-LUMO) and their attributes, such energy, are crucial. There are more significant functions for these orbitals in quantum chemistry. This also explains a range of reactions in conjugated systems and is used by the frontier electron density to forecast the most reactive region in π-electron systems [26]. A little space exists between the lowest unoccupied and highest occupied molecular orbitals (HOMO-LUMO) in conjugated compounds. The two molecular orbitals that most influence chemical stability are the lowest vacant and the highest occupied. The

capacity to provide an electron is represented by the HOMO, while the ability to receive an electron is represented by the LUMO, or electron acceptor. The following shows the HOMO and LUMO energies determined using the B3LYP/6-311++G(d,p) technique. One electron excitation from the highest occupied molecular orbital to the lowest unoccupied molecular orbital primarily describes this electronic absorption, which is associated with the transition from the ground to the first excited state. The electron affinity energy affects the LUMO energy, while the HOMO energy represents the ionization potential. The "energy gap" refers to the difference in orbitals between the LUMO and HOMO. It may be helpful in illuminating intramolecular charge transfer activity and is a necessary structural stability [27].

The molecular orbital energy values (HOMO and LUMO) provide useful information on the global reactivity descriptors. According to Koopmans' Theory, the ionization potential (I) and electron affinity (A) are expressed as IN [28].

I=-EHOMO and A=-ELUMO (1)

Using I and A values, the following expressions represent the electronegativity (χ), global chemical hardness (η), and electronic chemical potential (μ), respectively [29].

$\chi = (I+A)/2$, $\eta = (I-A)/2$, and $\mu = -(I+A)/2$ (2)

Global chemical softness (S) and electrophilicity index (ω) values are defined as follows [30].

$S = 1/\eta$ and $\omega = \mu^2/2\eta$ (3)

The calculated quantum parameters are summarized in Table 5.

TABLE 5 The ligand's theoretical global reactivity parameters

Parameters	Value
HOMO, (eV)	-6.653
LUMO, (eV)	-5.369
ΔE, (LUMO-HOMO gap) (eV)	1.284
Ionization potential (IP), (eV)	6.653
Electron affinity (A), (eV)	5.369
Hardness, (η) (eV)	0.642
Softness, (S) $(eV)^{-1}$	1.558
Electrophilicity (ω), (eV)	14.07
Chemical potential, (μ) (eV)	-6.011
Electronegativity, (χ) (eV)	6.011

To link the findings of the experimental investigation with the molecular structure and electronic characteristics of the ligand, a theoretical study at the B3LYP/6-311++G (d, p) level was conducted to complete the experimental study. The HOMO energy is often linked to a molecule's capacity to donate electrons to appropriate empty orbitals. Thus, by affecting the transfer process via the adsorbed layer, an increase in EHOMO values promotes adsorption. In contrast, the LUMO energy provides insight into the molecule's uptake of electrons. The molecule's capacity to take electrons from the iron surface is shown by a drop in the ELUMO value; the greater the inhibitory efficiency. It is well recognized from the literature that an effective corrosion inhibitor is often one that can both receive and release the electrons from the metal surface. The energy gap (Egap) is an additional crucial metric. Therefore, when the energy gap narrows, the adsorption Egap performance between the inhibitors and the metal surface rises. [31]. To gauge molecule stability and reactivity, chemical characteristics such as chemical hardness and softness are crucial. Therefore, as chemical reactivity rises, so does the adsorption inhibition efficiency; ordinarily, the molecule with the lowest hardness value should have the highest inhibition efficiency [32]. Due to the ligand compound's three active

centers- the atoms of sulfur, oxygen, and nitrogen- it effectively inhibits corrosion.

Molecular electrostatic potential (MEP)

When attempting to locate the active site in a system of molecules with a positive point charge, electrostatic potential is crucial. Positively charged organisms have a tendency to attack molecules with substantially negative electrostatic potentials (electrophilic attack). As demonstrated in Figures 4-8, the electrostatic potential of the free ligand was measure and projected as two-dimensional contours to determine the molecule's active site [33].

Conclusion

As a bidentate ligand, the ligand functions. The spectroscopic measurements demonstrate the coordination between the core transition metal ion and NH and the azomethane of heterocyclic groups. The transition metal complexes have been characterized using the susceptibility magnetic method. For the Ni(II) and Cu(II) complexes, a squarer, simpler shape is suggested; for the Co(II) complex, a tetrahedral geometry. The practical outcomes of the complexity sites were in good agreement with the findings of the electrostatic potential investigation. The concentration of the ligand determines how well it inhibits mild steel corrosion. The ligand is an effective corrosion inhibitor. It was discovered that the theoretical findings on the ligand inhibitor's ability to stop mild steel corrosion agreed with the experimental findings.

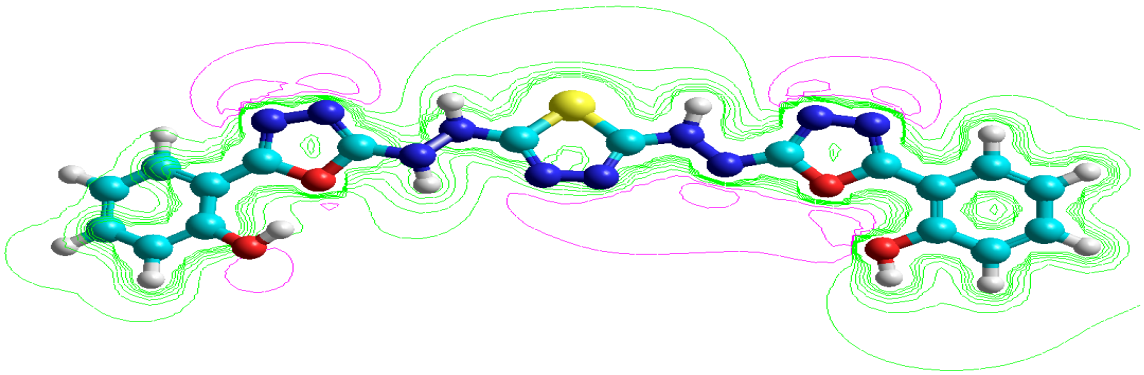

FIGURE 6 The electrostatic potential of HOMO as shapes for L

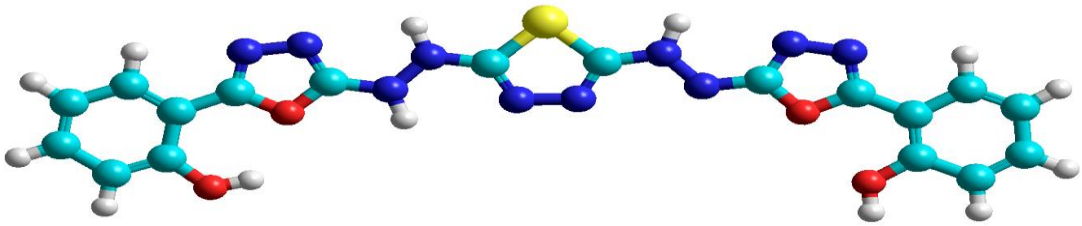

FIGURE 7 A visual representation of ligand's stereochemistry

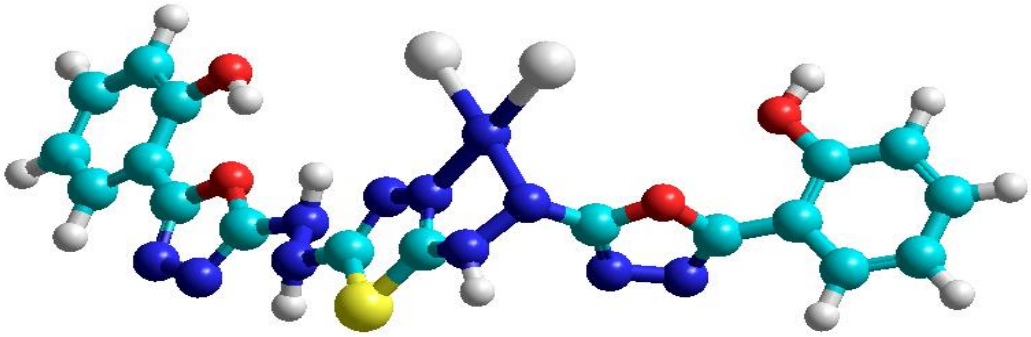

FIGURE 8 Stereochemistry of the compound [Co(L1)Cl2]

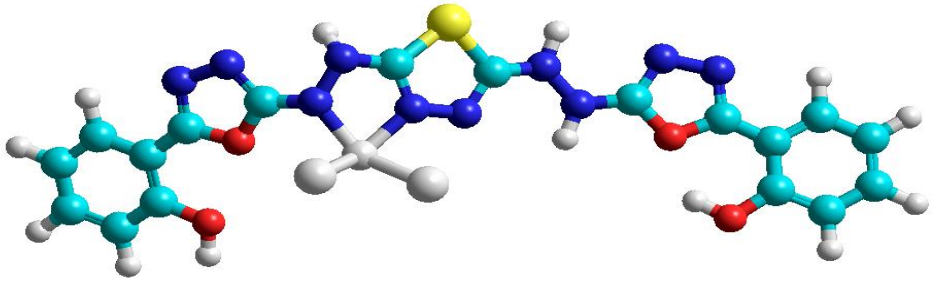

FIGURE 9 The stereochemistry of the compound [Ni(L1)Cl2]

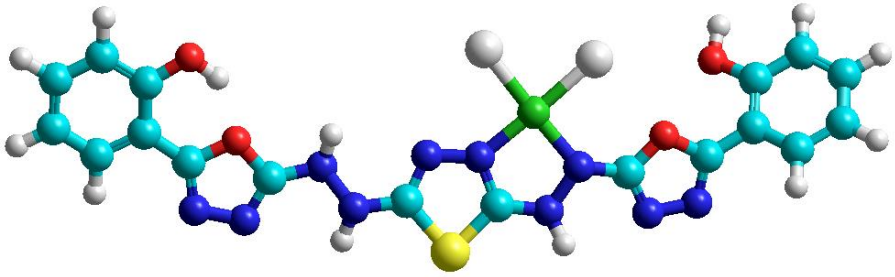

FIGURE 10 Stereochemistry of the compound [Cu(L1)Cl2]

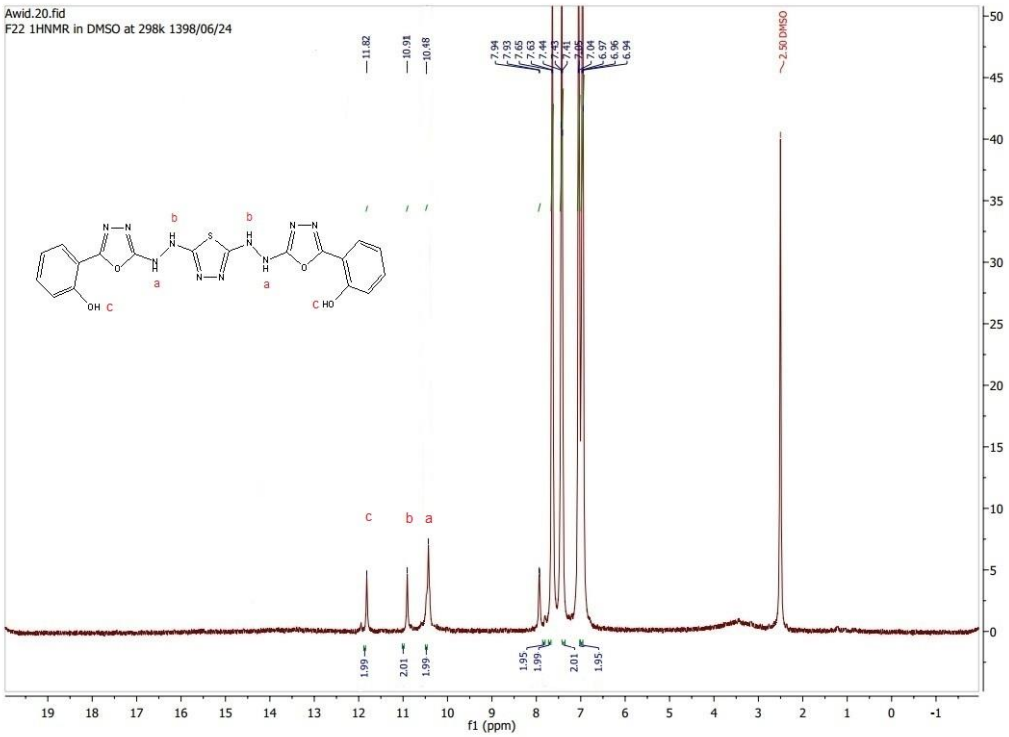

FIGURE 11 ^{1}H-NMR spectra of the ligand

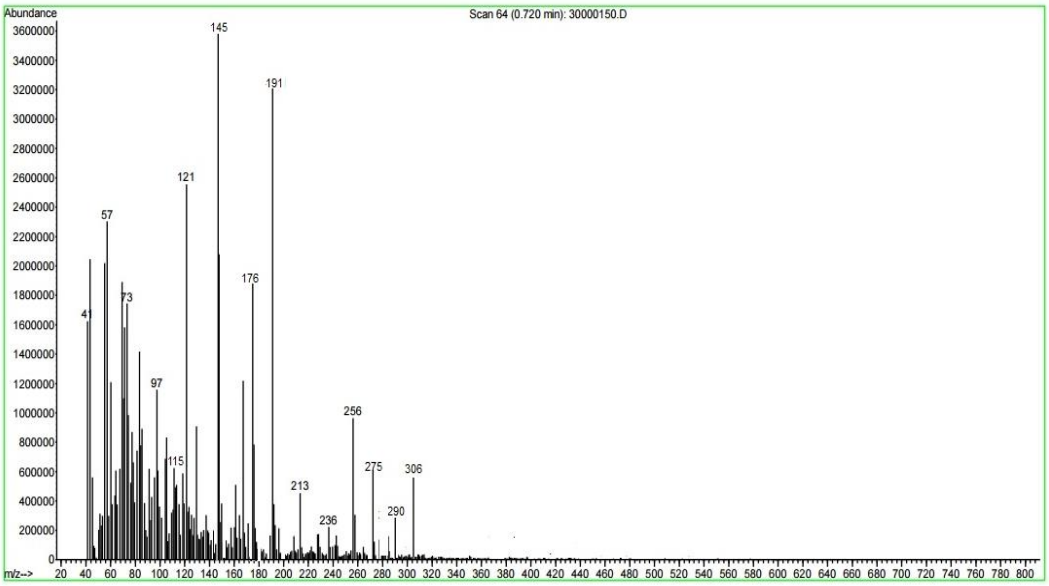

FIGURE 12 Mass spectra of ligand

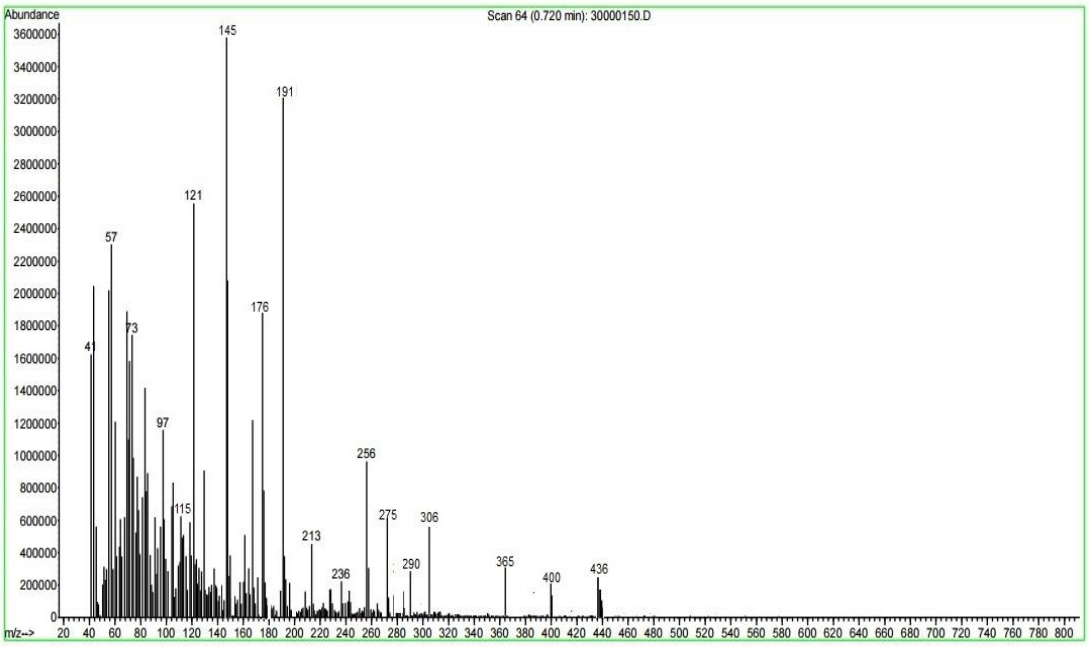

FIGURE 13 Mass spectra of [Co(L)Cl_2]

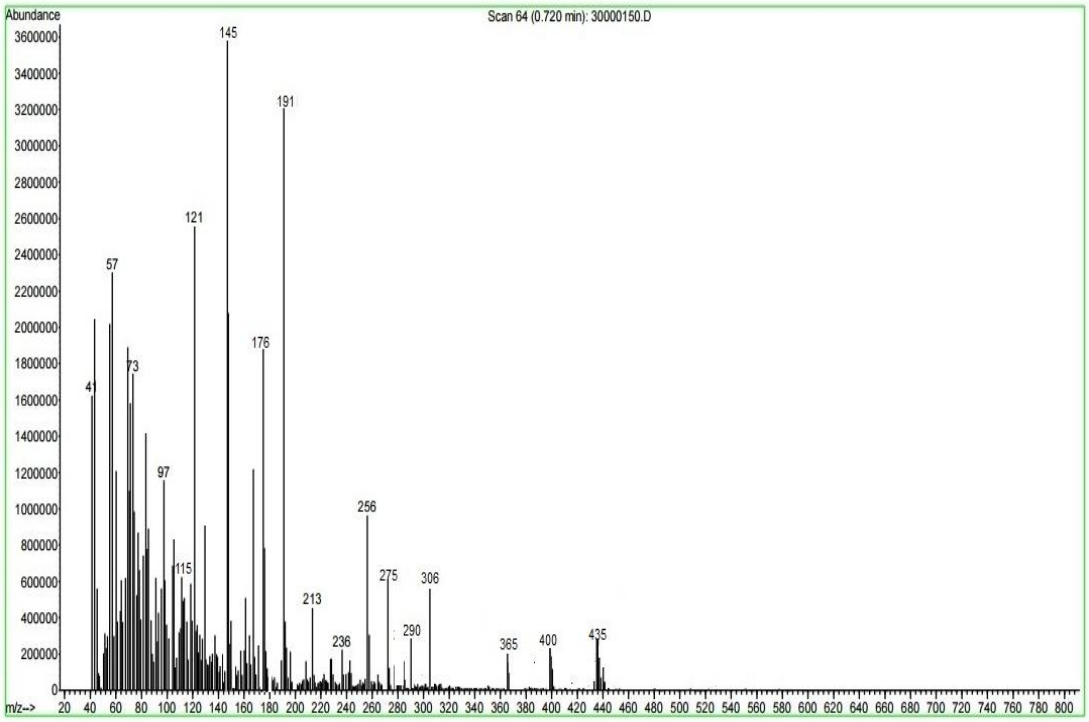

FIGURE 14 Mass spectra of [Cu(L)Cl2]

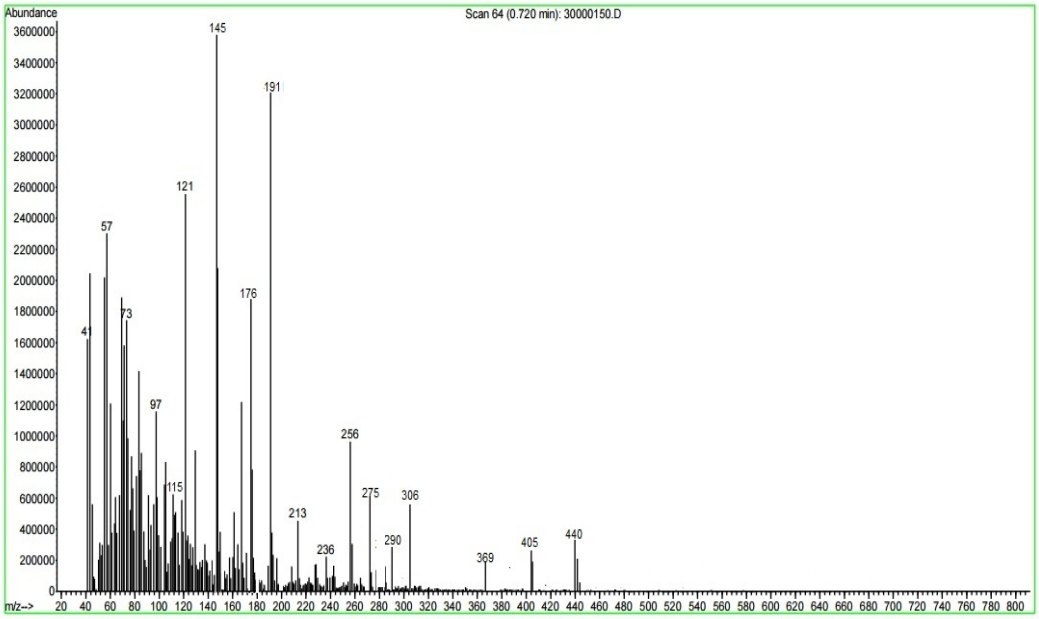

FIGURE 15 IR spectra of ligand

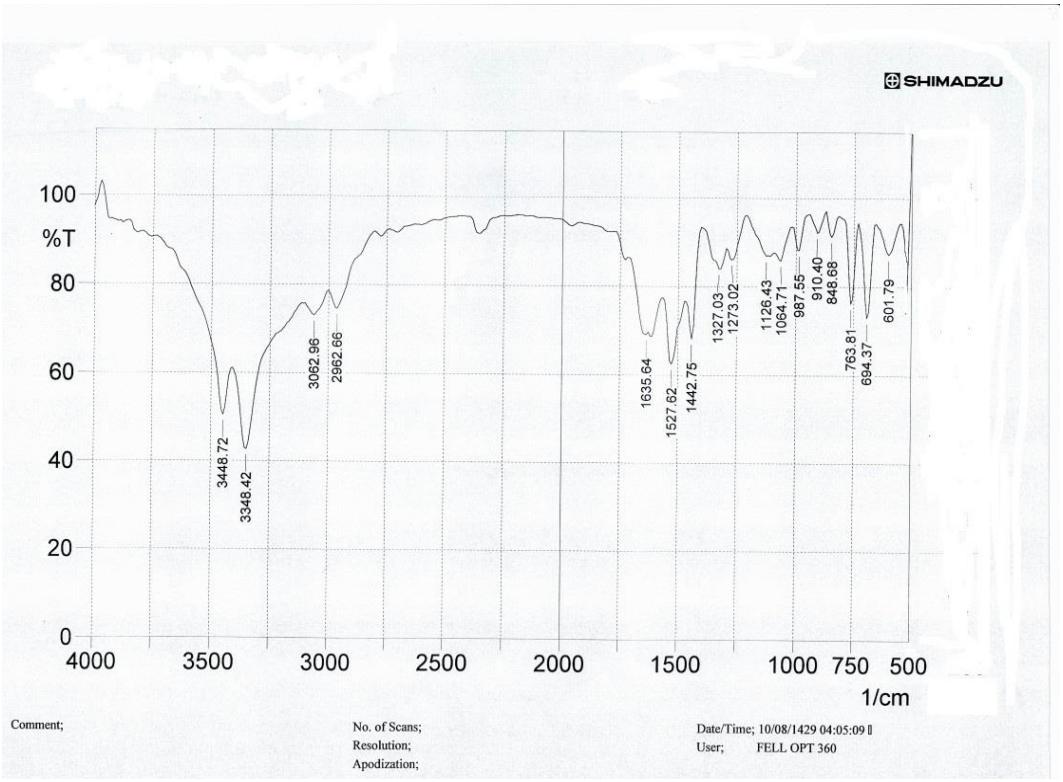

FIGURE 16 IR spectra of [Ni(L) Cl_2]

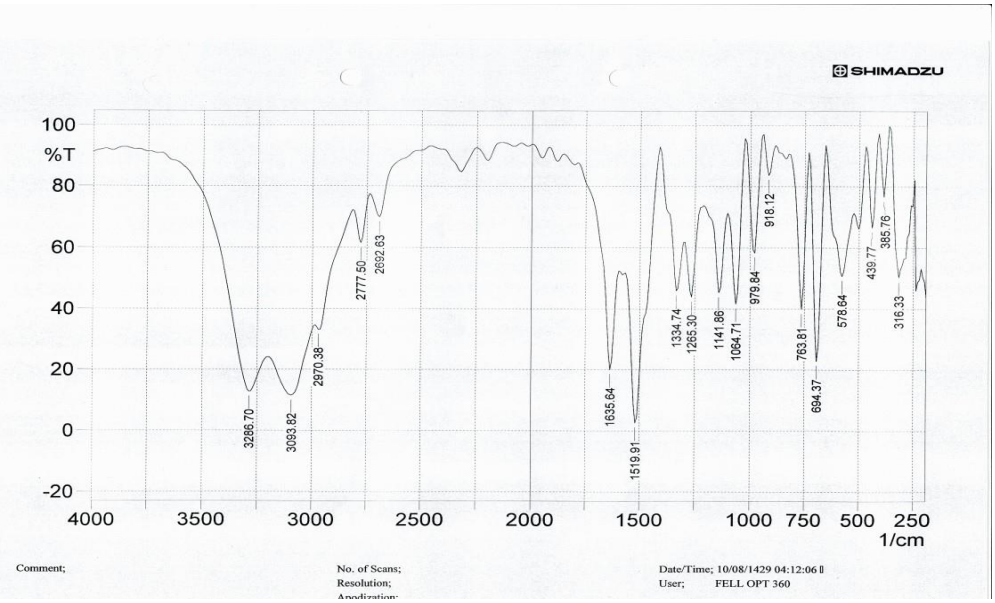

FIGURE 17 IR spectra of [Ni(L) Cl2]

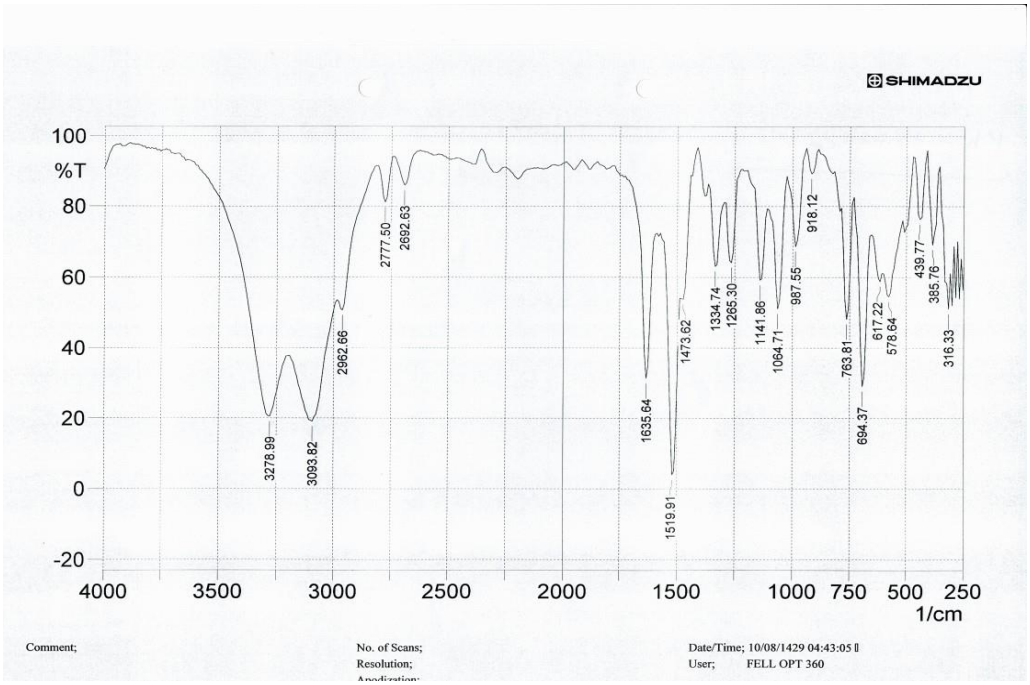

FIGURE 18 IR spectra of [Co(L) Cl2]

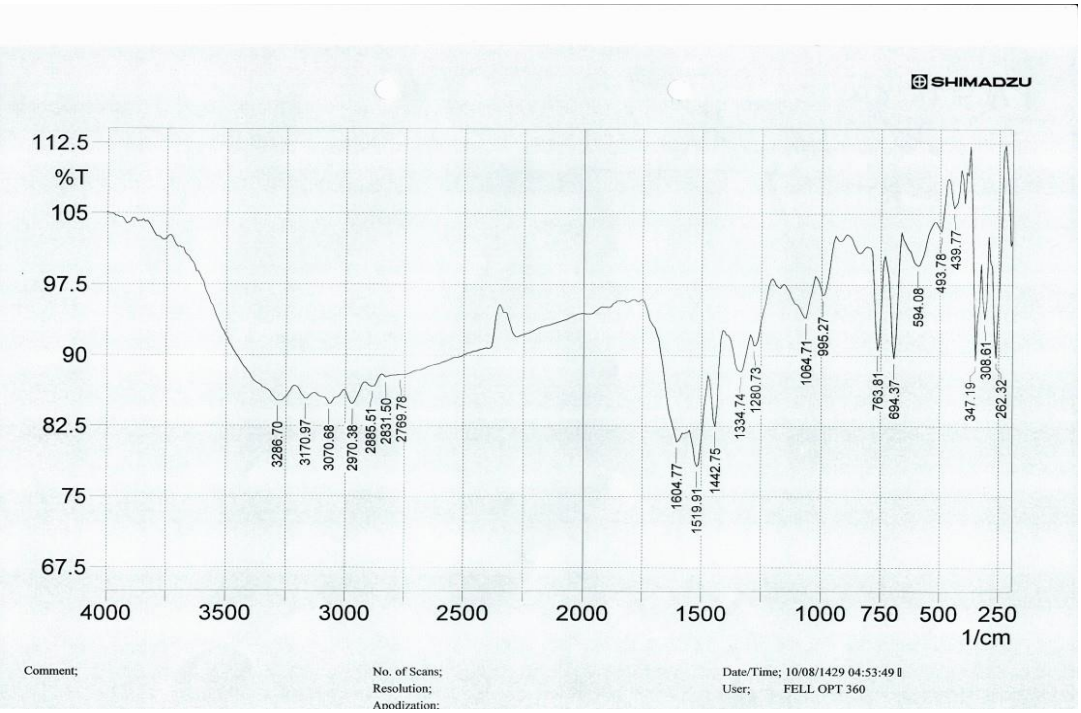

FIGURE 19 IR spectra of [Cu(L) Cl2]

Acknowledgements

The authors are grateful for the reviewer's valuable comments that improved the manuscript.

Funding

The authors state no funding involved.

Authors' Contributions

All authors have accepted responsibility for the entire content of this manuscript and approved its submission.

Conflict of Interest

The authors declare no conflict of interest.

Orcid:

Amal H. Anatheil:
https://orcid.org/0009-0009-5378-6354
Azhar Hameed Gatea:
https://orcid.org/0000-0002-4803-5494
Fayez Owaid Neamah:*
https://orcid.org/0009-0005-9812-7038

References

[1] a) F. Alam, B.K. Dey, Synthesis, characterization and in vitroanti-oxidant activity of some novel 1, 3, 4-thiadiazole derivatives, *Der Pharma Chemica*, **2015**, *7*, 230. [Google Scholar], [Publisher] ,b) C. Gholamrezazadeh, M. Hakimi, M. Dadmehr, A new and safe spirocyclic alkoxy phosphazene: Synthesis, characterization, DFT, molecular docking and photophysical properties, *Chemical Methodologies*, **2023**, *7*, 944-963. [Crossref], [Pdf], [Publisher], c) Y. Ghalandarzehi, H. Kord-Tamandani, Effect of solvents on kinetics and mechanistic investigation of highly substituted piperidines: Spectrometry approaches, *Asian Journal of Green Chemistry*, **2023**, *7*, 70-84. [Crossref], [Pdf], [Publisher], d) M. Mokhtary K. Mahooti, Recent advances in the synthesis of highly substituted piperidine analogs with biological activities, *Advanced Journal of Chemistry, Section A*, **2024**, *7*, 163-189. [Crossref], [Pdf], [Publisher]

[2] a) R. Aljabery, A. Gatea, I. Flifel, Synthesis,

characterization, antimicrobial studies of New5-[(2E)-2-{(2Z)-2-[2-(5-sulfanyl-1,3,4-thiadiazol-2-yl)hydrazinylidene]ethylidene}hydrazinyl]-1,3,4- thiadiazole-2-thioland their transition metal complexes, *International Journal of Pharmaceutical Research*, **2018**, *10*, 09752366. [Crossref], [Google Scholar], [Publisher], b) F. Khamooshi, S. Doraji-Bonjar, A.S. Akinnawo, H. Ghaznavi, A.R. Salimi-Khorashad, M.J. Khamooshi, Dark classics in chemical neuroscience: Comprehensive study on the biochemical mechanisms and clinical implications of opioid analgesics, *Chemical Methodologies*, **2023**, *7*, 964-993. [Crossref], [Pdf], [Publisher], c) M. Asif, S. Alghamdi, Antitubercular drugs: new drugs designed by molecular modifications, *Asian Journal of Green Chemistry*, **2022**, *6*, 327-354. [Crossref], [Pdf], [Publisher], d) T.A. Nyijime, H.F. Chahul, A.M. Ayuba, F. Iorhuna, Theoretical investigations on thiadiazole derivatives as corrosion inhibitors on mild steel, *Advanced Journal of Chemistry, Section A*, **2023**, *6*, 141-154. [Crossref], [Pdf], [Publisher]

[3] A. Gatea, Synthesis, characterization, antimicrobial of studies new 2, 2'-{(1Z, 2Z) ethane-1, 2 diylidenebis [(2Z) hydrazin-1-yl-2-ylidene-1, 3, 4 oxadiazole-5, 2-diyl]} diphenol and their transition metal complexes, *Journal of Global Pharma Technology*, **2018**, *10*, 102-111. [Google Scholar], [Publisher]

[4] A. Al-Haidari, E. Al-Tamimi, Synthesis of new derivatives of 1,3,4-thiadiazole and 1,3,4-oxadiazole on cyclic imides and studying their antioxidant, *Eurasian Chemical Communications*, **2021**, *3*, 508-517. [Crossref], [Google Scholar], [Publisher]

[5] J. Patil, Versatile applications of heterocyclic compounds: special attention to nanomaterials in cancer therapy, *Journal of Pharmacovigilance*, **2016**, *4*, 1-2. [Crossref], [Google Scholar], [Publisher]

[6] A. Mittal, Synthetic nitroimidazoles: biological activities and mutagenicity relationships, *Scientia Pharmaceutica*, **2009**, *77*, 497-520. [Crossref], [Google Scholar], [Publisher]

[7] G. Nagalakshmi, Synthesis, antimicrobial and antiinflammatory activity of 2, 5-disubstituted-1, 3, 4-oxadiazoles, *Indian Journal of Pharmaceutical Sciences*, **2008**, *70*, 49. [Crossref], [Google Scholar], [Publisher]

[8] M.Hossain, A.K. Nanda, A review on heterocyclic: synthesis and their application in medicinal chemistry of imidazole moiety, *Science*, **2018**, *6*, 83-94. [Google Scholar], [Publisher]

[9] P. Arora, V. Arora, H.S. Lamba, D. Wadhwa, Importance of heterocyclic chemistry: a review, *International Journal of Pharmaceutical Sciences and Research*, **2012**, *3*, 2947. [Google Scholar], [Publisher]

[10] A.H. Anatheil, A. Hameed, W.S. Abdulredhad, A review on heterocyclic and their application in chemistry of coumarin moiety, *ResearchJet Journal of Analysis and Inventions*, **2022**, *3*, 1-12. [Crossref], [Pdf], [Publisher]

[11] D.A. Najeeb, Some Transition Metal Complexes with 2-thioacetic acid-5-pyridyl-1,3,4-oxadiazol, *Al-Nahrain Journal of Science*, **2011**, *14*, 35–39. [Crossref], [Google Scholar], [Publisher]

[12] K.K. Jha, A. Samad, Y. Kumar, M. Shaharyar, R.L. Khosa, J. Jain, V. Kumar, P. Singh, Design, synthesis and biological evaluation of 1, 3, 4-oxadiazole derivatives, *European Journal of Medicinal Chemistry*, **2010**, *45*, 4963-4967. [Crossref], [Google Scholar], [Publisher]

[13] E. Yousif, E. Bakir, J. Salimon, N. Salih, Evaluation of Schiff bases of 2,5-dimercapto-1,3,4-thiadiazole as photostabilizer for poly(methyl methacrylate), *Journal of Saudi Chemical Society*, **2012**, *16*, 279-285. [Crossref], [Google Scholar], [Publisher]

[14] A.M. Al-Azzawi, A.S. Hamd, Synthesis, characterization and evaluation of biological activity of novel cyclic imides containing heterocycles based on 2, 5 disubstituted-1, 3, 4-thiadiazoles, *Al-Anbar Journal of Veterinary*

Sciences, **2011**, *4*, 152-164. [Google Scholar], [Publisher]

[15] C. Anghel, M. Matache, C.C. Paraschivescu, A.M. Madalan, M. Andruh, A novel 1-D coordination polymer constructed from disilver-1,3,4-oxadiazole nodes and perchlorato bridges, *Inorganic Chemistry Communications*, **2017**, *76*, 22–25. [Crossref], [Google Scholar], [Publisher]

[16] X.B. Zhang, B.C. Tang, P. Zhang, M. Li, W.J. Tian, Synthesis and characterization of 1, 3, 4-oxadiazole derivatives containing alkoxy chains with different lengths, *Journal of Molecular Structure*, **2007**, *846*, 55-64. [Crossref], [Google Scholar], [Publisher]

[17] P. Aggarwal, B.Singh, A. Paul, Pore size and electronic tuning in cerium-doped CoFe-LDH for the oxygen evolution reaction, *Materials Advances*, **2023**, *4*, 4377-4389. [Crossref], [Google Scholar], [Publisher]

[18] K.J. AL-Adilee, A.K. Abass, A.M. Taher, Synthesis of some transition metal complexes with new heterocyclic thiazolyl azo dye and their uses as sensitizers in photo reactions, *Journal of Molecular Structure*, **2016**, *1108*, 378-397. [Crossref], [Google Scholar], [Publisher]

[19] K.J. AL-Adilee, A.K. Abass, A.M. Taher, Synthesis of some transition metal complexes with new heterocyclic thiazolyl azo dye and their uses as sensitizers in photo reactions, *Journal of Molecular Structure*, **2016**, *1108*, 378-397. [Crossref], [Google Scholar], [Publisher]

[20] M.H. Hussein, M.F. El-Hady, H.A. Shehata, M.A. Hegazy, H.H. Hefni, Preparation of some eco-friendly corrosion inhibitors having antibacterial activity from sea food waste, *Journal of Surfactants and Detergents*, **2013**, *16*, 233-242. [Crossref], [Google Scholar], [Publisher]

[21] Ł. Cieśla, J. Kryszeń, A. Stochmal, W. Oleszek, M. Waksmundzka-Hajnos, Approach to develop a standardized TLC-DPPH test for assessing free radical scavenging properties of selected phenolic compounds, *Journal of Pharmaceutical and Biomedical Analysis*, **2012**, *70*, 126-135. [Crossref], [Google Scholar], [Publisher]

[22] F. Bentiss, M. Traisnel, H. Vezin, H.F. Hildebrand, M. Lagrenee, 2, 5-Bis (4-dimethylaminophenyl)-1, 3, 4-oxadiazole and 2, 5-bis (4-dimethylaminophenyl)-1, 3, 4-thiadiazole as corrosion inhibitors for mild steel in acidic media, *Corrosion Science*, **2004** *46*, 2781-2792. [Crossref], [Google Scholar], [Publisher]

[23] A.A. Rahim, E. Rocca, J. Steinmetz, M.J. Kassim, R. Adnan, M.S. Ibrahim, Mangrove tannins and their flavanoid monomers as alternative steel corrosion inhibitors in acidic medium, *Corrosion Science*, **2007**, *49*, 402-417. [Crossref], [Google Scholar], [Publisher]

[24] W.J. Hehre, Ab initio molecular orbital theory, *Accounts of Chemical Research*, **1976**, *9*, 399-406. [Crossref], [Google Scholar], [Publisher]

[25] V.V.V. Hugo, H.S.M. Alejandro, V.S.A. María, R.H. María, L.R.M. Antonio, P.O.M. Guadalupe, Á. Enrique, Molecular Modeling and Synthesis of Ethyl Benzyl Carbamates as Possible Ixodicide Activity, *Computational Chemistry*, **2018**, *7*, 1-26. [Crossref], [Google Scholar], [Publisher]

[26] C.H. Choi, M. Kertesz, Conformational information from vibrational spectra of styrene, trans-stilbene, and cis-stilbene, *The Journal of Physical Chemistry A*, **1997**, *101*, 3823-3831. [Crossref], [Google Scholar], [Publisher]

[27] L. Padmaja, C. Ravikumar, D. Sajan, I. Hubert Joe, V.S. Jayakumar, G.R. Pettit, O. Faurskov Nielsen, Density functional study on the structural conformations and intramolecular charge transfer from the vibrational spectra of the anticancer drug combretastatin-A2, *Journal of Raman Spectroscopy: An International Journal for Original Work in all Aspects of Raman Spectroscopy, Including Higher Order Processes,*

and also Brillouin and Rayleigh Scattering, 2009, *40*, 419-428. [Crossref], [Google Scholar], [Publisher]

[28] T. Koopmans, Über die Zuordnung von Wellenfunktionen und Eigenwerten zu den einzelnen Elektronen eines Atoms, *Physica A: Statistical Mechanics and its Applications*, **1934**, *1*, 104-113. [Google Scholar], [Publisher]

[29] L.H. Mendoza-Huizar, A theoretical study of chemical reactivity of tartrazine through DFT reactivity descriptors, *Journal of the Mexican Chemical Society*, **2014**, *58*, 416-423. [Google Scholar], [Publisher]

[30] R. Ustabaş, N. Süleymanoğlu, Y. Ünver, Ş. Direkel, 5-(4-Bromobenzyl)-4-(4-(5-phenyl-1,3,4-oxadiazole-2-yl)phenyl)-2,4-dihydro-3H-1,2,4-triazole-3-one: Synthesis, characterization, DFT study and antimicrobial activity, *Journal of Molecular Structure*, **2020**, *1214*, 128217. [Crossref], [Google Scholar], [Publisher]

[31] R. Yıldız, An electrochemical and theoretical evaluation of 4, 6-diamino-2-pyrimidinethiol as a corrosion inhibitor for mild steel in HCl solutions, *Corrosion Science*, **2015**, *90*, 544-553. [Crossref], [Google Scholar], [Publisher]

[32] K. Ramya, R. Mohan, A. Joseph, Adsorption and electrochemical studies on the synergistic interaction of alkyl benzimadazoles and ethylene thiourea pair on mild steel in hydrochloric acid, *Journal of the Taiwan Institute of Chemical Engineers*, **2014**, *45*, 3021-3032. [Crossref], [Google Scholar], [Publisher]

[33] R.F. Hout, W.J. Pietro, W.J. Hehre, A pictorial approach to molecular structure and reactivity. *(No Title)*, **1984**. [Google Scholar], [Publisher]

How to cite this article: Amal H. Anatheil, Azhar Hameed Gatea, Fayez Owaid Neamah*, Synthesis, characterization, anticorrosion, and computational study of new thiadiazole-oxadiazole derivatives with some transition metal ion. *Journal of Medicinal and Pharmaceutical Chemistry Research*, 2024, 6(8), 1149-1166. **Link:** https://jmpcr.samipubco.com/article_193247.html